

Cite this: *Chem. Sci.*, 2025, 16, 5849

All publication charges for this article have been paid for by the Royal Society of Chemistry

## Photocatalytic 1,3-difluoroalkylcarboxylation of alkenes by triple kinetic-controlled radical self-ordering†

Hong Fu, Zuo-Shuai Wang, Si-Jia Li, Lin-Yuan Zhu, Xiao-Jian Wang, Hong-Chen Wang and Bing Han \*

A transition-metal-free protocol for the unsymmetrical radical 1,3-difunctionalization of alkenes has been established for the first time in the form of 1,3-difluoroalkylcarboxylation by a photocatalytic radical three-component reaction of allyl formates, trifluoroacetanilides, and cesium formate. This reaction employs formate as the carboxylating reagent and trifluoroacetanilide as the difluoroalkylating reagent via C–F bond activation. As a result, a series of previously inaccessible unsymmetrical difluorinated adipic acid derivatives can be easily and efficiently prepared. Mechanism studies reveal that triple kinetic-controlled radical self-ordering is the key to this unique reaction. This radical sorting involves the fast initiation of a CO<sub>2</sub> radical anion and its chemoselective addition and reduction, followed by the slow generation of a fluoroalkyl radical and its chemo-/regioselective addition. Notably, this strategy is also suitable for the 1,3-difluoroalkylcarboxylation of unsymmetrical and cyclic alkenes through diastereoselectively constructing two or three consecutive stereocenters.

Received 20th December 2024

Accepted 18th February 2025

DOI: 10.1039/d4sc08607d

rsc.li/chemical-science

As a common class of chemicals with a wide range of sources, the diverse conversion reactions of olefins provide a convenient and practical way to obtain high-value-added functional molecules. Among these conversions, 1,2-difunctionalization is the one of the most representative modes, as it affords a convenient method for simultaneously introducing two functional groups and has received extensive attention.<sup>1</sup> Both symmetrical and unsymmetrical 1,2-difunctionalization reactions have been fully developed by introducing two identical or different functional groups, respectively (Scheme 1A).<sup>2,3</sup> Recently, the 1,3-difunctionalization of olefins has become a hot research topic because it provides a facile method to obtain useful 1,3-difunctionalized moieties through an unusual remote functionalization of alkene (Scheme 1B).<sup>4</sup> Several practical strategies have been established, which can be divided into two-electron and one-electron processes. The positional isomerization of olefins mediated by transition metal hydride intermediates is the dominant method of the former, and the precious metal Pd and the coinage metal Ni have proven to be the most effective catalysts in these conversions.<sup>5</sup> Metal-free 2e processes have also been developed using high-valence iodine as the oxidizing reagent, which involve ionic rearrangement facilitated by I<sup>(III)</sup>,

leading to the 1,3-difluorination of olefins.<sup>6</sup> Conversely, with the emergence of increasingly efficient and controllable radical initiation methods, olefin 1,3-difunctionalization reactions involving one-electron processes have gradually been developed. One elegant approach is to use radical 1,2-functional group (FG) migration as a key link to realize a variant 1,3-difunctionalization in the form of a 1,2,3-trifunctionalization.<sup>7</sup> Some successful examples have employed 1,2-boron,<sup>7a</sup> 1,2-acyl,<sup>7b–d</sup> and 1,2-aryl<sup>7e</sup> migrations. In addition, the radical addition/elimination/re-addition (AERA) strategy has also proven to be a promising protocol.<sup>8</sup> Consequently, some symmetric 1,3-difunctionalizations are realized, such as dicarboxylation,<sup>8a</sup> difluoroalkylation,<sup>8b</sup> diaminoalkylation<sup>8c</sup> and diphosphination.<sup>8d</sup> Although these approaches widen the range of olefin 1,3-difunctionalizations, most are limited to the symmetrical pattern, while their unsymmetrical counterparts, especially for the 1e-process, remain an unrealized goal.

As the radical AERA strategy affords a viable method for symmetrical 1,3-difunctionalization, it is expected to be applicable to unsymmetrical reactions as well. Despite this expectation, it presents a formidable challenge, as the process is bound to involve multiple competitive reactions due to the employment of two different radicals. These competitions result in the disordered radical additions of the two radicals to the substrate alkenes and the derived alkene intermediates, as well as undesired radical cross-coupling.<sup>9</sup> Thus, both symmetrical and unsymmetrical 1,3-difunctionalizations and the unwanted cross-coupled adducts would be produced as a complex

State Key Laboratory of Applied Organic Chemistry (SKLAOC), College of Chemistry and Chemical Engineering, Lanzhou University, 222 South Tianshui Road, Lanzhou, 730000, People's Republic of China. E-mail: hanb@lzu.edu.cn

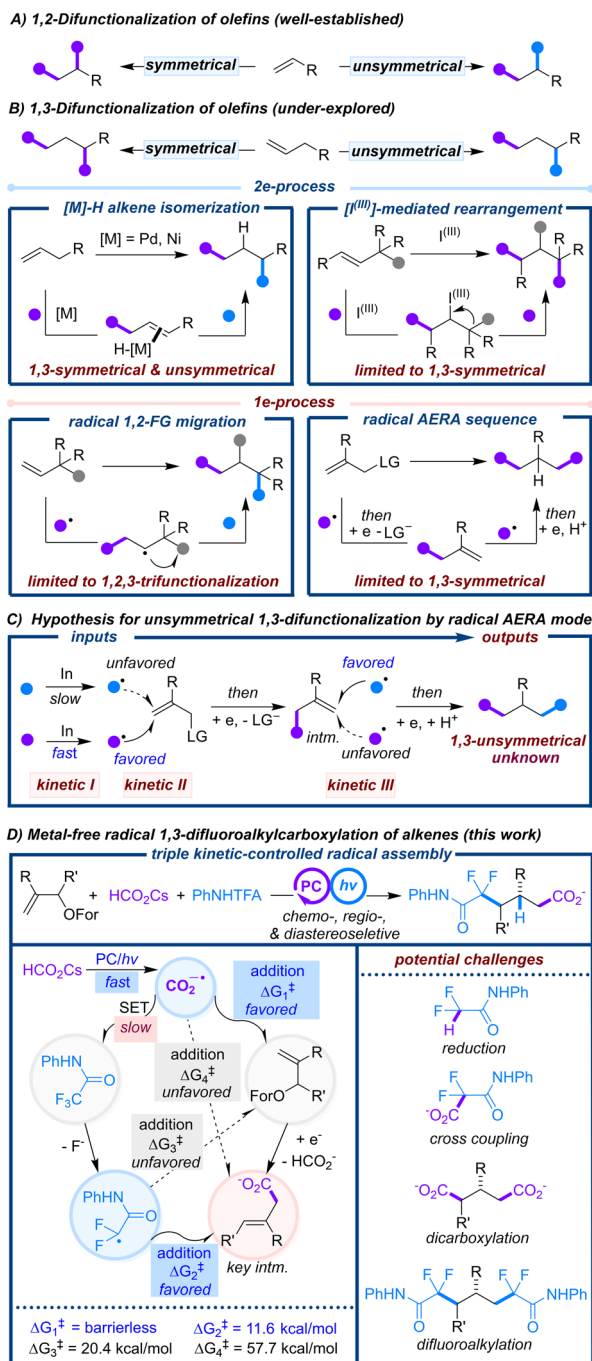
† Electronic supplementary information (ESI) available. CCDC 2381321 and 2381323. For ESI and crystallographic data in CIF or other electronic format see DOI: <https://doi.org/10.1039/d4sc08607d>



mixture. To obtain the desired 1,3-unsymmetrical product while avoiding the formation of other byproducts, a triple kinetic-controlled process was hypothesized; this process depends on several factors (Scheme 1C). First, a significant rate difference is necessary for the generation of two kinds of radicals to be applied (kinetic I). Secondly, the radical species produced first should have a faster addition rate to the substrate alkene than the other, slow-forming radical species to obtain a single intermediate alkene (kinetic II). Thirdly, the slow-forming radical should have kinetic selectivity toward preferential

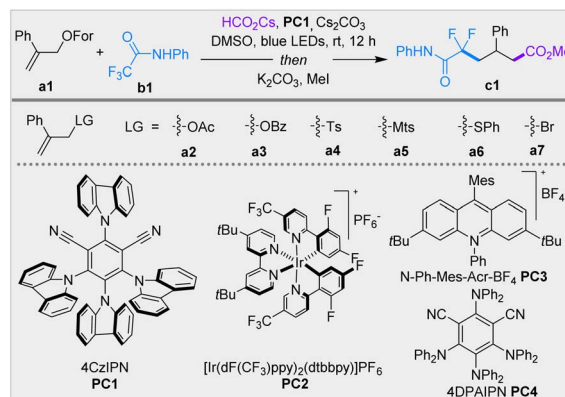
addition to the derived intermediate alkene rather than the substrate alkene (kinetic III). Finally, the cross-coupling between these two radicals should be much slower than their addition to the corresponding alkenes.

Herein, we realize this hypothesis in the form of the radical 1,3-difluoroalkylcarboxylation of olefins by a photocatalytic three-component reaction of allyl formates, trifluoroacetanilides, and cesium formate (Scheme 1D). To the best of our knowledge, this protocol represents the first successful example of unsymmetrical 1,3-difunctionalization *via* a 1e-process. This approach initiates from the photocatalytic oxidation of formate to generate a carbon dioxide radical anion ( $\text{CO}_2^{\cdot-}$ ),<sup>10</sup> which preferentially reacts with allyl formates through fast radical addition. The nascent tertiary radical would be converted to the key intermediate but-3-enoate by subsequent reduction and further elimination of a formate anion.<sup>11,8b</sup> With the consumption of allyl formate and the accumulation of but-3-enoate,  $\text{CO}_2^{\cdot-}$  begins to reduce trifluoroacetanilide to a difluoroacetanilide radical *via* C-F bond activation.<sup>12</sup> The latter preferentially adds to but-3-enoate rather than allyl



Scheme 1 1,3-Difunctionalization of olefins.

Table 1 Optimization of the reaction conditions



Entry	Variation of conditions <sup>a</sup>	Yield <sup>b</sup>
1	None	60%
2	<b>a2</b> instead of <b>a1</b>	23%
3	<b>a3, a4, a6, a7</b> instead of <b>a1</b>	<10%
4	<b>a5</b> instead of <b>a1</b>	26%
5	$\text{HCO}_2\text{Na}$ instead of $\text{HCO}_2\text{Cs}$	41%
6	Without $\text{Cs}_2\text{CO}_3$	45%
7	DMF instead of DMSO	28%
8	<b>PC2</b> instead of <b>PC1</b>	Trace
9	<b>PC3</b> instead of <b>PC1</b>	Trace
10	<b>PC4</b> instead of <b>PC1</b>	52%
11	3 eq. of <b>b1</b>	51%
12	1.5 eq. of <b>b1</b>	23%
13	<b>Under CO<sub>2</sub> atmosphere</b>	<b>68%</b>
14	$\text{CO}_2$ atmosphere instead of $\text{HCO}_2\text{Cs}$	NR
15	Without <b>PC1</b>	NR
16	In the dark	NR

<sup>a</sup> Reaction conditions: **a1** (0.2 mmol, 1 eq.), **b1** (4 eq.),  $\text{HCO}_2\text{Cs}$  (2 eq.),  $\text{Cs}_2\text{CO}_3$  (0.5 eq.), 4CzIPN (**PC1**, 2 mol%), DMSO (3 mL), Ar, blue LEDs (425 nm, 30 W), rt, 12 h; then MeI (0.3 mL) and  $\text{K}_2\text{CO}_3$  (1.0 mmol), rt, 4 h. <sup>b</sup> Isolated yield.



formate by taking advantage of the kinetic rate difference. Finally, the radical 1,3-difluoroalkylcarboxylation is achieved by this triple kinetic amplification process. As a result, a series of previously inaccessible unsymmetrical difluorinated adipic acid derivatives can be easily prepared using this convenient photocatalytic multi-component reaction. Adipic acid derivatives are very useful structural units and play important roles in organic synthesis and polymerization.<sup>13</sup> In this context, this protocol not only successfully extends the radical AERA sequence to 1,3-unsymmetrical difunctionalization of olefins but also provides a simple method toward significant moieties.

The study was commenced by stirring allyl formate **a1**, trifluoroacetanilide **b1**, cesium formate, and cesium carbonate in dimethylsulfoxide (DMSO) under irradiation by blue LEDs (425 nm, 30 W) at room temperature under an argon atmosphere. When 4CzIPN was used as the photocatalyst, the 1,3-difluoroalkylcarboxylation took place smoothly and gave the desired product **c1** in 60% yield (Table 1, entry 1). Formate proved to be the best leaving group (LG); when **a2–a7**, which contained OAc, OBz, Ts, trimethylphenylsulphonyl (Mts), thiophenyl, and Br groups, were tested, the reaction gave unsatisfactory yields (entries 2–4).<sup>14</sup> When sodium formate was used instead of cesium formate as the reactant and reductant, the reaction yield was reduced to 41% (entry 5). Cesium carbonate was essential for efficient reaction, as the yield of **c1** dropped dramatically in its absence (entry 6). When DMF was used instead of DMSO, **c1** was obtained in only 28% yield (entry 7). Other photocatalysts, namely, [Ir(dF(CF<sub>3</sub>)ppy)<sub>2</sub>(dtbbpy)]PF<sub>6</sub> (**PC2**), *N*-Ph-Mes-Acr-BF<sub>4</sub> (**PC3**), and 4DPAIPN (**PC4**), were also tested, but they were ineffective except for **PC4**, which provided **c1** in 52% yield (entries 8–10). The amount of **b1** used also influenced the reaction efficiency, as when it was decreased to 3 equiv. and 1.5 equiv., the yield of **c1** was reduced to 51% and 23%, respectively (entries 11 and 12). Additionally, the yield of **c1** was slightly increased to 68% when the reaction was performed under a CO<sub>2</sub> atmosphere (entry 13), whereas no reaction took place when the reaction was conducted under a CO<sub>2</sub> atmosphere without the addition of cesium formate (entry 14), implying that cesium formate is crucial for efficient reaction, and a CO<sub>2</sub> atmosphere is merely conducive to promoting the reaction, but not a decisive factor. Notably, no reaction occurred when the reaction was performed without **PC1** or without light irradiation (entries 15 and 16).

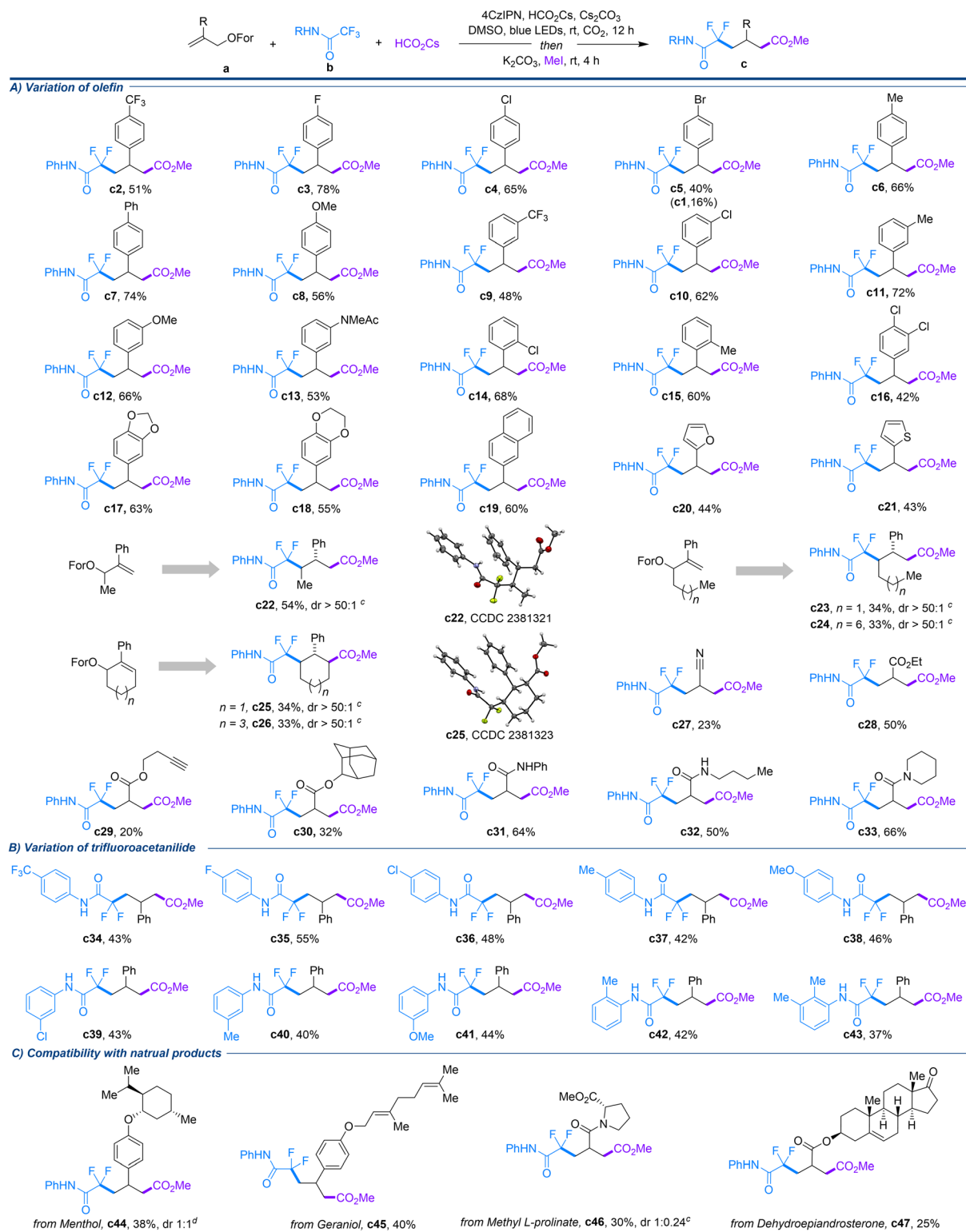
With the optimal conditions in hand (entry 13 in Table 1), the reaction scope was investigated, and the results are shown in Scheme 2. The allyl formate scope was first investigated (Scheme 2A). 2-Phenylallyl formates bearing *para*-substituents with a wide range of electronic properties, such as trifluoromethyl, fluorine, chlorine, bromine, methyl, phenyl, and methoxy groups, were all converted smoothly in the reaction, providing the desired products **c2–c8** in good yields. When the *para*-bromophenyl functionalized allyl formate was used in the reaction, in addition to the normal product **c5**, which was obtained in 40% yield, **c1** was also formed in 16% yield. The formation of **c1** can be attributed to the fact that **c5** is prone to further reductive debromination under the reaction conditions.<sup>15</sup> In addition, *meta*-substituted 2-phenylallyl formates

bearing electron-deficient or electron-donating groups, such as trifluoromethyl, chlorine, methyl, methoxy, and acetamido groups, on the phenyl ring exhibited good compatibility with the protocol, delivering products **c9–c13** in moderate-to-good yields. Similarly, this approach was also suitable for *ortho*-substituted phenyl counterparts, as demonstrated in the cases of **c14** and **c15**, which produced the corresponding products in good yields. Notably, olefins containing disubstituted phenyl moieties, such as 2,3-dichlorophenyl, 3,4-piperonyl, and 3,4-ethylenedioxyphenyl moieties, were also good candidates for the transformation, affording products **c16–c18** in good yields. In addition to phenyl, olefins incorporating other aromatic and heteroaromatic groups, such as naphthalene, furan and thiophene, were also well tolerated in the method, giving **c19–c21** in moderate yields. Significantly, when unsymmetrical alkenes with different chain lengths were subjected to the reaction, the regio- and diastereoselective 1,3-difluoroalkylcarboxylation took place smoothly, providing products **c22–c24** in moderate yields as a single diastereomer. The structure and the *anti*-configuration of **c22** were confirmed through an X-ray diffraction study. The excellent regioselectivity of the unsymmetrical olefins indicates that the addition of CO<sub>2</sub><sup>•−</sup> rather than the difluoroalkyl radical onto the allyl formate is the key step. In addition, allyl formates involving cyclic alkenes, such as cyclohexene and cyclooctene, were also suitable for this protocol. Through regio- and diastereoselective processes, **c25** and **c26** were produced as a single diastereomer with three continuous chiral centers in 34% and 33% yields, respectively. The structure and the adjacent *trans*-configuration of the three continuous stereocenters of **c25** were confirmed through an X-ray diffraction study. It is noteworthy that when the aromatic ring moiety of the allyl formates was replaced by electron-deficient groups such as cyano, ester and amide groups, the reaction still proceeded smoothly, providing the corresponding products **c27–c33** in moderate-to-good yields. The functional group tolerance of this approach is also fully demonstrated by the incorporation of functional groups such as esters, amides, and alkynes into the allyl moiety.

Next, the scope of the trifluoroacetamides was tested, as shown in Scheme 2B. *N*-Phenylamides containing *para*-substituents with a variety of electronic properties, such as CF<sub>3</sub>, F, Cl, Me, and MeO, were all suitable for the conversion, providing the corresponding products **c34–c38** in moderate yields. In addition, *N*-phenylamides containing *meta*-/*ortho*-substituents were also good partners for this method, as illustrated by **c39–c43**. To investigate the compatibility of the protocol for complex skeletons, allyl formates containing natural products, including terpenes, an amino acid, and a steroid, were tested in the approach as well. As illustrated in Scheme 2C, the scaffolds of menthol, geraniol, L-proline, and dehydroepiandrosterone were all compatible in the reaction, producing the corresponding products **c44–c47** in moderate yields.

To further prove the practicability of this strategy, a gram-scale preparation reaction was conducted, as shown in Scheme 3. Reaction on a 6 mmol scale using **a1** proceeded successfully and gave 1.19 g of the product **c1** (57% yield). The



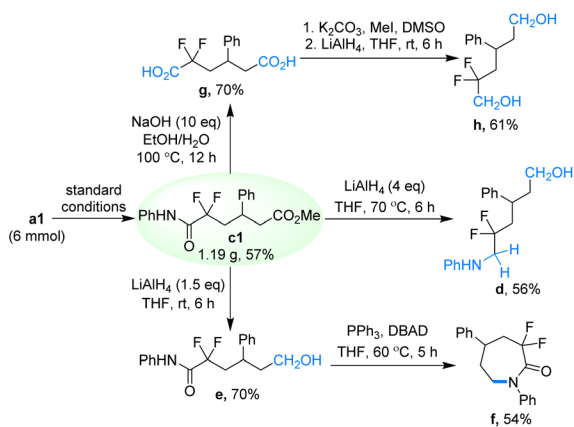


**Scheme 2** Exploration of substrate scope.<sup>a,b</sup> <sup>a</sup>Reaction conditions: **a** (0.2 mmol, 1 eq.), **b** (4 eq.), HCO<sub>2</sub>Cs (2 eq.), Cs<sub>2</sub>CO<sub>3</sub> (0.5 eq.), 4CzIPN (2 mol%), DMSO (3 mL), CO<sub>2</sub> (1 atm), blue LEDs (425 nm, 30 W), rt, 12 h; then MeI (0.3 mL), K<sub>2</sub>CO<sub>3</sub> (2.0 mmol), rt, 4 h. <sup>b</sup>Isolated yield. <sup>c</sup>The diastereomer ratio was determined by <sup>1</sup>H NMR. <sup>d</sup>The diastereomer ratio was determined by <sup>19</sup>F NMR.

usefulness of the product was also demonstrated by subsequent derivatization to provide various difluoro-containing key intermediates, as shown in Scheme 3. When **c1** was treated with

different amounts of LiAlH<sub>4</sub> at room temperature or under heating, the gradient reduction of **c1** could be easily achieved by generating the full and partial reductive deoxygenation



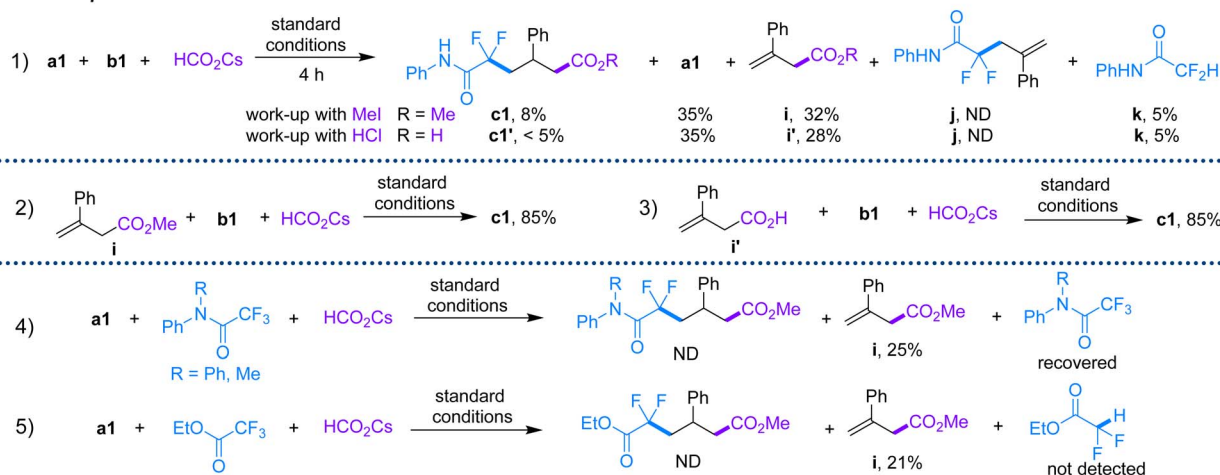


Scheme 3 Gram-scale synthesis and follow-up conversions.

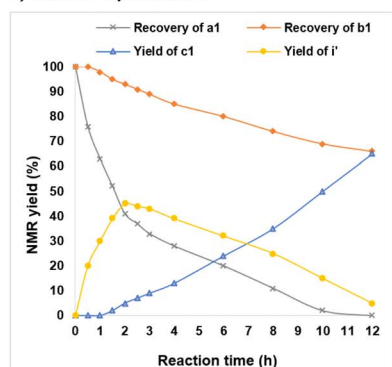
products **d** and **e** in 56% and 70% yields, respectively. The latter could be further converted to  $\alpha,\alpha$ -difluoro-*N*-phenylcaprolactam **f** in 54% yield under Mitsunobu reaction conditions. Hydrolysis of **c1** under basic conditions gave  $\alpha,\alpha$ -difluoro-adipic acid **g** in 70% yield, which could be further reduced to  $\alpha,\alpha$ -difluorohexanediol **h** in 61% yield.

To further understand the mechanism of this reaction, control experiments, fluorescence quenching experiments and kinetic experiments were performed, as shown in Scheme 4. When the reaction time was shortened to 4 h under the standard conditions, **c1** was obtained in only 8% yield and **a1** was recovered in 35% yield, accompanied by the formation of methyl but-3-enoate **i** and difluoroacetanilide **k** in 32% and 5% yields, respectively (Scheme 4A-1). In addition, when the aforementioned reaction was treated with HCl as a work-up process, the corresponding but-3-enoic acid **i'** was also obtained in 28% yield. By treating ester **i** or acid **i'** with **b1** under the standard conditions, the desired product **c1** was obtained in 85% yield in both reactions (Scheme 4A-2 and 3). Apparently, but-3-enoate is the key intermediate of the reaction, which is produced by the fast addition of the generated  $\text{CO}_2^{2-}$  to allyl formate. In addition, the formation of a tiny amount of **k** and **c1** also implies that the fluoroalkyl radical is slowly produced and preferentially added to the intermediate alkene but-3-enoate rather than to allyl formate. This view is also confirmed by the lack of detection of possible intermediate **j**. However, when ethyl trifluoroacetate and *N,N*-disubstituted trifluoroacetanilide were used instead of **b1** for the reaction under standard conditions, they were totally recovered, and only

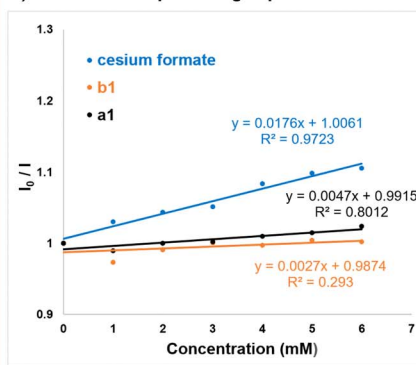
## A) Control experiments



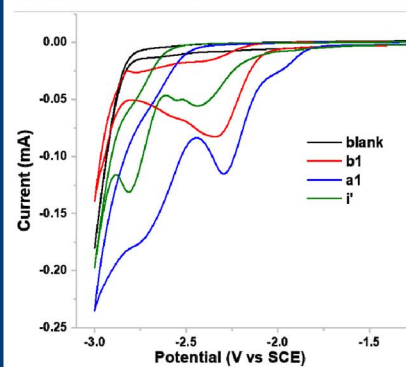
## B) Kinetic experiments



## C) Stern-Volmer quenching experiments

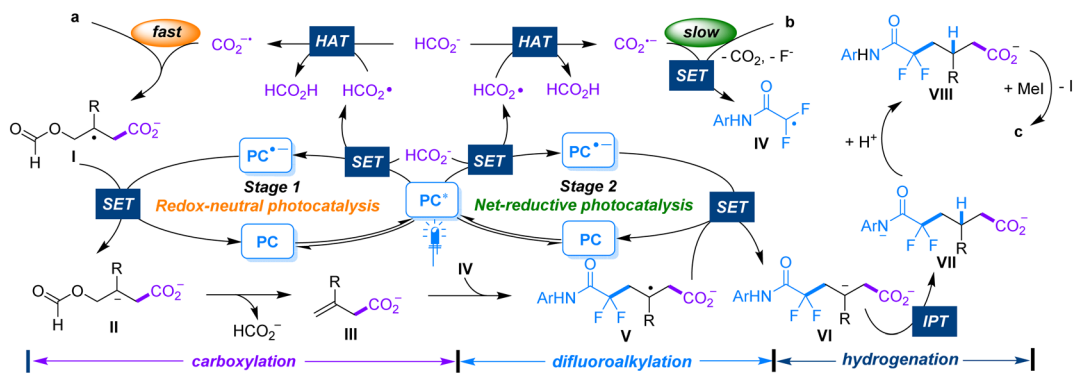


## D) Cyclic voltammetry experiments



Scheme 4 Mechanistic studies.





Scheme 5 Proposed mechanism.

intermediate **i** was obtained (Schemes 4A-4 and 5). These results suggest that the N–H moiety of **b** is critical for the reaction, as it is probably involved in the spin-centre shift promoted reductive defluorination of trifluoroacetanilide<sup>12</sup> and final intramolecular proton transfer.<sup>16</sup> This triple kinetic-controlled reaction is apparently crucial for the efficient unsymmetrical 1,3-difunctionalization, which is also confirmed by the reaction rate curves as illustrated in Scheme 4B. Moreover, fluorescence quenching experiments showed that the excited  $PC1^*$  could be significantly quenched by cesium formate, but was hardly quenched by **a1** and **b1** (Scheme 4C). These results not only indicate that the reaction begins from the photoredox of formate by the excited state of  $PC1$  but also verifies that  $CO_2^{\cdot-}$  is produced first in the reaction. Unlike in Yu's strategy, in which formate derived *in situ* from the reduction of  $CO_2$  by sacrificing an equivalent of  $Ph_3SiH$  acts as a carboxylation reagent,<sup>7e</sup> formate is used directly as the carboxylation reagent as well as the reductant in this study. Although the cyclic voltammogram illustrated in Scheme 4D implies that **a1** ( $E_{1/2} = -2.13$  V vs. SCE) could also be continuously reduced by  $CO_2^{\cdot-}$  ( $E_{1/2} = -2.2$  V vs. SCE) to an allylic carbanion to further add to  $CO_2$  to form the key intermediate but-3-enoate (see ESI† for a possible alternative path), this process is obviously not a significant path, because, as shown in entry 1 of Table 1, the reaction could also occur efficiently without  $CO_2$ . This result indicates that the formation of but-3-enoate is more likely to involve the addition of  $CO_2^{\cdot-}$  to allylic formate rather than reduction by it. In addition, the obtained reductive potentials of **b1** ( $E_{1/2} = -2.18$  V vs. SCE) and but-3-enoate ( $E_{1/2} = -2.30$  V vs. SCE) suggest that the former could indeed be reduced by  $CO_2^{\cdot-}$ , whereas the reduction of the latter does not seem easy. In addition, DFT (density functional theory) calculation results also confirm that the proposed kinetic-controlled process of the addition of  $CO_2^{\cdot-}$  to allyl formates is barrierless, but its addition to the intermediate but-3-enoate is a very difficult process with an extremely high energy barrier of  $57.7$  kcal mol<sup>-1</sup>. In contrast, the addition of a fluoroalkyl radical to but-3-enoate is favorable and only requires crossing an energy barrier of  $11.6$  kcal mol<sup>-1</sup>, while its addition to allyl formates is unfavorable and requires crossing an energy barrier of  $20.4$  kcal mol<sup>-1</sup> (see ESI† for details of DFT calculations).

Based on our experimental observations and previous reports in the literature,<sup>16,17,8b</sup> a plausible mechanism involving a two-stage photocatalytic cycle is illustrated in Scheme 5. The reaction is initiated by the photooxidation of formate ( $E_{1/2} = +0.93$  V vs. SCE for  $HCO_2^-/HCO_2^{\cdot}$ )<sup>10c</sup> by the excited  $PC1^*$  ( $E_{1/2} = +1.35$  V vs. SCE for  $PC^*/PC^{\cdot-}$ )<sup>18</sup> to produce  $PC^{\cdot-}$  and a formoxyl radical *via* a single-electron transfer (SET) process. Hydrogen atom transfer (HAT) between the formoxyl radical and formate would give formic acid and  $CO_2^{\cdot-}$ . The latter adds rapidly to substrate **a** *via* a barrierless process to provide the radical intermediate **I**. **I** would be further reduced by  $PC^{\cdot-}$  to the carbanion intermediate **II**, which immediately eliminates formate through C–O bond cleavage to yield intermediate **III** accompanied by the regeneration of  $PC$  (stage 1). Conversely, with the consumption of substrate **a** and accumulation of intermediate **III**,  $CO_2^{\cdot-}$  begins to reduce substrate **b**. Through SET reduction and subsequent defluorination-facilitated spin-centre transfer, **b** is converted to the radical **IV**. **IV** tends to add to the key intermediate **III** to provide radical **V**, which is further reduced by  $PC^{\cdot-}$  to give the intermediate **VI** (stage 2). **VI** immediately undergoes intramolecular proton transfer (IPT)<sup>16</sup> from the tethered N–H to the carbanion center to form the intermediate **VII**, which subsequently abstracts a proton from the surroundings to yield the intermediate **VIII**. Finally, after treatment with MeI, **VIII** is methylated to produce the desired product **c**.

In summary, a transition-metal free protocol for the 1,3-difluoroalkylcarboxylation of alkenes has been established for the first time *via* a photocatalytic three-component reaction of allyl formates, trifluoroacetanilides, and cesium formate. This approach employs 4CzIPN as a cost-effective organic photocatalyst, formate as a carboxylating reagent, and trifluoroacetanilides as the difluoroalkylating reagent. Consequently, a series of structurally useful difluorinated adipic acid derivatives were efficiently produced. This chemistry represents the first successful example of the unsymmetrical 1,3-difunctionalization of alkenes *via* a 1e-process as well as the first unsymmetrical extension of the radical AERA strategy. The triple kinetic-controlled radical self-ordering is the crucial key to the success of the protocol, which involves the sequential production of  $CO_2^{\cdot-}$  and difluoromethylaniline radicals and



their chemo-/regioselective additions to alkenes. This strategy not only broadens the boundaries of radical AERA strategy but also provides a new tactic for the unsymmetrical 1,3-difunctionalization of olefins. Other 1,3-unsymmetrical difunctionalizations of olefins are being explored in our groups.

## Data availability

The ESI† includes all experimental details, including synthesis and characterization of all starting materials and products reported in this study, and mechanistic studies. NMR spectra of all products reported are included as well.

## Author contributions

B. H. and H. F. conceived and directed the project. H. F., S. L., L. Z., X. W. and H. W. performed experiments. H. F., S. L., L. Z. and X. W. prepared the ESI.† Z. W. performed the DFT calculations and drafted the DFT parts. B. H. wrote the paper. All authors discussed the results and commented on the manuscript.

## Conflicts of interest

There are no conflicts to declare.

## Acknowledgements

We thank the National Natural Science Foundation of China (No. 22471109, 22171118, and 21873041) and the Science and Technology Major Program of Gansu Province of China (22ZD6FA006, 23ZDFA015, and 24ZD13FA017) for financial support.

## Notes and references

- For selected reviews, see: (a) H.-M. Huang, P. Bellotti, J. Ma, T. Dalton and F. Glorius, *Nat. Rev. Chem.*, 2021, **5**, 301–321; (b) H. Jiang and A. Studer, *Chem. Soc. Rev.*, 2020, **49**, 1790–1811; (c) L. M. Wickham and R. Giri, *Acc. Chem. Res.*, 2021, **54**, 3415–3437; (d) S. Zhu, X. Zhao, H. Li and L. Chu, *Chem. Soc. Rev.*, 2021, **50**, 10836–10856; (e) J. Derosa, O. Apolinar, T. Kang, V. T. Tran and K. M. Engle, *Chem. Sci.*, 2020, **11**, 4287–4296; (f) X. Bao, J. Li, W. Jiang and C. Huo, *Synthesis*, 2019, **51**, 4507–4530.
- For selected works, see: (a) N. Fu, G. S. Sauer and S. Lin, *J. Am. Chem. Soc.*, 2017, **139**, 15548–15553; (b) Q. Wu, A. Roy, E. Irran, Z.-W. Qu, S. Grimme, H. F. T. Klare and M. Oestreich, *Angew. Chem., Int. Ed.*, 2019, **58**, 17307–17311; (c) B. Tian, P. Chen, X. Leng and G. Liu, *Nat. Catal.*, 2021, **4**, 172–179; (d) T. Ju, Y.-Q. Zhou, K.-G. Cao, Q. Fu, J.-H. Ye, G.-Q. Sun, X.-F. Liu, L. Chen, L.-L. Liao and D.-G. Yu, *Nat. Catal.*, 2021, **4**, 304–311; (e) L. Liu, M. C. Aguilera, W. Lee, C. R. Youshaw, M. L. Neidig and O. Gutierrez, *Science*, 2021, **374**, 432–439; (f) X. Hu, I. Cheng-Sánchez, W. Kong, G. A. Molander and C. Nevado, *Nat. Catal.*, 2024, **7**, 655–665; (g) J. Z. Wang, W. L. Lyon and D. W. C. MacMillan, *Nature*, 2024, **628**, 104–109.
- Our work for difunctionalization of olefins. (a) S.-Q. Lai, B.-Y. Wei, J.-W. Wang, W. Yu and B. Han, *Angew. Chem., Int. Ed.*, 2021, **60**, 21997–22003; (b) D. Wei, T. Liu, Y. He, B. Wei, J. Pan, J. Zhang, N. Jiao and B. Han, *Angew. Chem., Int. Ed.*, 2021, **60**, 26308–6313; (c) D.-T. Xie, H.-L. Chen, D. Wei, B.-Y. Wei, Z.-H. Li, J.-W. Zhang, W. Yu and B. Han, *Angew. Chem., Int. Ed.*, 2022, **61**, e202203398; (d) S.-P. Hu, C.-H. Gao, T.-M. Liu, B.-Y. Miao, H.-C. Wang, W. Yu and B. Han, *Angew. Chem., Int. Ed.*, 2024, **63**, e202400168.
- (a) R. K. Dhungana, R. R. Sapkota, D. Niroula and R. Giri, *Chem. Sci.*, 2020, **11**, 9757–9774; (b) D.-K. Wang, L. Li, Q. Xu, J. Zhang, H. Zheng and W.-T. Wei, *Org. Chem. Front.*, 2021, **8**, 7037–7049; (c) X. Ma, Q. Zhang and W. Zhang, *Molecules*, 2023, **28**, 3027–3072.
- (a) H. Sommer, F. Juliá-Hernández, R. Martin and I. Marek, *ACS Cent. Sci.*, 2018, **4**, 153–165; (b) Y. Li, D. Wu, H. Cheng and G. Yin, *Angew. Chem., Int. Ed.*, 2020, **59**, 7990–8003; (c) H.-Y. Tu, S. Zhu, F.-L. Qing and L. Chu, *Synthesis*, 2020, **52**, 1346–1356; (d) W. Li, J. K. Boon and Y. Zhao, *Chem. Sci.*, 2018, **9**, 600–607; (e) Z. Wu, J. Meng, H. Liu, Y. Li, X. Zhang and W. Zhang, *Nat. Chem.*, 2023, **15**, 988–997.
- (a) H. A. Sharma, K. M. Mennie, E. E. Kwan and E. N. Jacobsen, *J. Am. Chem. Soc.*, 2020, **142**, 16090–16096; (b) A. C. Dean, E. H. Randle, A. J. D. Lacey, G. A. M. Giorio, S. Doobary, B. D. Cons and A. J. J. Lennox, *Angew. Chem., Int. Ed.*, 2024, **63**, e202404666.
- (a) K. Jana, A. Bhunia and A. Studer, *Chem*, 2020, **6**, 512–522; (b) R. Liu, Y. Tian, J. Wang, Z. Wang, X. Li, C. Zhao, R. Yao, S. Li, L. Yuan, J. Yang and D. Shi, *Sci. Adv.*, 2022, **8**, eabq8596; (c) H. -Z. Xiao, B. Yu, S. -S. Yan, W. Zhang, X. -X. Li, Y. Bao, S. -P. Luo, J. -H. Ye and D. -G. Yu, *Chin. J. Catal.*, 2023, **50**, 222–228; (d) G. Zhao, S. Lim, D. G. Musaev and M.-Y. Ngai, *J. Am. Chem. Soc.*, 2023, **145**, 8275–8284; (e) H. -Z. Xiao, B. Yu, S. -S. Yan, W. Zhang, X. -X. Li, Y. Bao, S. -P. Luo, J. -H. Ye and D. -G. Yu, *Chin. J. Catal.*, 2023, **50**, 222–228.
- (a) Z. Yao, G. Li, Y. Zhou, L. Xu and D. Xue, *Adv. Synth. Catal.*, 2023, **365**, 224–229; (b) B. Yu, Y. Liu, H.-Z. Xiao, S.-R. Zhang, C.-K. Ran, L. Song, Y.-X. Jiang, C.-F. Li, J.-H. Ye and D.-G. Yu, *Chem*, 2024, **10**, 938–951; (c) X.-Y. Wang, P. Xu, W.-W. Liu, H.-Q. Jiang, S.-L. Zhu, D. Guo and X. Zhu, *Sci. China: Chem.*, 2024, **67**, 368–373; (d) H. Xin, L. Zhang, J. Liao, X.-H. Duan, X. Yang and L.-N. Guo, *Org. Lett.*, 2024, **26**, 6030–6034; (e) J.-X. Yu, Y.-Y. Cheng, X.-Y. Zeng, B. Chen, C.-H. Tung and L.-Z. Wu, *Org. Lett.*, 2024, **26**, 6809–6813; (f) W. Shan, Z. Wang, C. Gao, X. Li, W. Zhuang, R. Liu, C. Shi, H. Qin, X. Li and D. Shi, *Green Chem.*, 2024, **26**, 9749–9756.
- (a) M. Uno, S. Sumino, T. Fukuyama, M. Matsuura, Y. Kuroki, Y. Kishikawa and I. Ryu, *J. Org. Chem.*, 2019, **84**, 9330–9338; (b) H. Li and S. Chiba, *Chem Catal.*, 2022, **2**, 1128–1142; (c) E. L. Saux, M. Zanini and P. Melchiorre, *J. Am. Chem. Soc.*, 2022, **144**, 1113–1118.
- (a) J. Majhi and G. A. Molander, *Angew. Chem., Int. Ed.*, 2024, **63**, e202311853; (b) W. Xiao, J. Zhang and J. Wu, *ACS Catal.*, 2023, **13**, 15991–16011; (c) Y. Huang, J. Hou, L.-W. Zhan, Q. Zhang, W.-Y. Tang and B.-D. Li, *ACS Catal.*, 2021, **11**, 15004–15012; (d) S. N. Alektiar, J. Han, Y. Dang,



- C. Z. Rubel and Z. K. Wickens, *J. Am. Chem. Soc.*, 2023, **145**, 10991–10997; (e) S. N. Alektiar and Z. K. Wickens, *J. Am. Chem. Soc.*, 2021, **143**, 13022–13028.
- 11 (a) W. Zhang and S. Lin, *J. Am. Chem. Soc.*, 2020, **142**, 20661–20670; (b) F.-L. Haut, R. S. Mega, J. V. Estornell and R. Martin, *Angew. Chem., Int. Ed.*, 2023, **62**, e202304084; (c) S. Senapati, S. K. Parida, S. S. Karandikar and S. Murarka, *Org. Lett.*, 2023, **25**, 7900–7905.
- 12 (a) Y.-J. Yu, F.-L. Zhang, T.-Y. Peng, C.-L. Wang, J. Cheng, C. Chen, K. N. Houk and Y.-F. Wang, *Science*, 2021, **371**, 1232–1240; (b) S.-S. Yan, S.-H. Liu, L. Chen, Z.-Y. Bo, K. Jing, T.-Y. Gao, B. Yu, Y. Lan, S.-P. Luo and D.-G. Yu, *Chem*, 2021, **7**, 3099–3113; (c) M. W. Campbell, V. C. Polites, S. Patel, J. E. Lipson, J. Majhi and G. A. Molander, *J. Am. Chem. Soc.*, 2021, **143**, 19648–19654; (d) J.-H. Ye, P. Bellotti, C. Heusel and F. Glorius, *Angew. Chem., Int. Ed.*, 2022, **61**, e202115456.
- 13 (a) Y. Wan and J.-M. Lee, *ACS Catal.*, 2021, **11**, 2524–2560; (b) J. Rios, J. Lebeau, T. Yang, S. Li and M. D. Lynch, *Green Chem.*, 2021, **23**, 3172–3190; (c) J. Yang, J. Liu, H. Neumann, R. Franke, R. Jackstell and M. Beller, *Science*, 2019, **366**, 1514–1517.
- 14 (a) J. Zhang, Y. Li, R. Xu and Y. Chen, *Angew. Chem., Int. Ed.*, 2017, **56**, 12619–12623; (b) K. Sun, M. Ueno, K. Imaeda, K. Ueno, M. Sawamura and Y. Shimizu, *ACS Catal.*, 2021, **11**, 9722–9728; (c) Y. Zhou, Y. Qin, Q. Wang, Z. Zhang and G. Zhu, *Angew. Chem., Int. Ed.*, 2022, **61**, e202110864; (d) X. Chen, X. Luo and P. Wang, *Tetrahedron Lett.*, 2022, **91**, 153646.
- 15 (a) A. J. Boyington, C. P. Seath, A. M. Zearfoss, Z. Xu and N. T. Jui, *J. Am. Chem. Soc.*, 2019, **141**, 4147–4153; (b) A. F. Chmiel, O. P. Williams, C. P. Chernowsky, C. S. Yeung and Z. K. Wickens, *J. Am. Chem. Soc.*, 2021, **143**, 10882–10889; (c) C. M. Hendy, G. C. Smith, Z. Xu, T. Lian and N. T. Jui, *J. Am. Chem. Soc.*, 2021, **143**, 8987–8992.
- 16 P. Lei, B. Chen, T. Zhang, Q. Chen, L. Xuan, H. Wang, Q. Yan, W. Wang, J. Zeng and F. Chen, *Org. Chem. Front.*, 2024, **11**, 458–465.
- 17 (a) A. M. Vasquez, J. A. Gurak Jr, C. L. Joe, E. C. Cherney and K. M. Engle, *J. Am. Chem. Soc.*, 2020, **142**, 10477–10484; (b) Z. Wu, S. N. Gockel and K. L. Hull, *Nat. Commun.*, 2021, **12**, 5956; (c) J.-T. Li, G. Fang, G.-Y. Wu and C.-X. Zhuo, *ACS Catal.*, 2023, **13**, 12648–12655.
- 18 Y. Liu, X.-L. Chen, X.-Y. Li, S.-S. Zhu, S.-J. Li, Y. Song, L.-B. Qu and B. Yu, *J. Am. Chem. Soc.*, 2021, **143**, 964–972.

